Equilibration Dynamics of Strongly Interacting Bosons in 2D Lattices with Disorder

Mi Yan, Hoi-Yin Hui, Marcos Rigol, and V. W. Scarola

Equilibration Dynamics of Strongly Interacting Bosons in 2D Lattices with Disorder

Mi Yan,[1] Hoi-Yin Hui,[1] Marcos Rigol,[2] and V.W. Scarola[1]

[1]*Department of Physics, Virginia Tech, Blacksburg, VA 24061, USA*
[2]*Department of Physics, The Pennsylvania State University, University Park, PA 16802, USA*
(Dated: July 21, 2017)

Motivated by recent optical lattice experiments [Choi et al., Science **352**, 1547 (2016)], we study the dynamics of strongly interacting bosons in the presence of disorder in two dimensions. We show that Gutzwiller mean-field theory (GMFT) captures the main experimental observations, which are a result of the competition between disorder and interactions. Our findings highlight the difficulty in distinguishing glassy dynamics, which can be captured by GMFT, and many-body localization, which cannot be captured by GMFT, and indicate the need for further experimental studies of this system.

Introduction: Ultracold atoms loaded into optical lattices [1–3] offer ideal platforms to study localization [4, 5]. Examples in the noninteracting limit include fermionic band insulators [6], and, in the presence of (quasi-)disorder, Anderson insulators [7–12]. In clean systems, localization can also occur because of interactions, producing Mott insulators (MIs) [13–17]. Recent experimental studies have explored the interplay between disorder and interactions [18–28]. In the ground state of bosonic systems, this interplay can generate the Bose-glass (BG) phase [29, 30]. The BG, like the bosonic MI, is characterized by a vanishing superfluid density but, unlike the MI, it is compressible. At extensive energy densities above the ground state, the interplay between disorder and interactions can lead to a remarkable phenomenon known as many-body localization (MBL) [31–33]. In the MBL phase, eigenstate thermalization [34–36] does not occur [37].

Signatures of MBL were recently observed with fermions [26, 27] and bosons in two dimensions (2D) [28]. Our work is motivated by the latter experiment (see Refs. [38, 39] for theoretical studies inspired by the former). In Ref. [28], a MI with one boson per site was prepared in a harmonic trap in a deep optical lattice. All bosons in one half of the system were then removed and the remaining half was allowed to evolve by lowering the lattice depth, with or without disorder. During the dynamics, the parity-projected occupation of the lattice sites was measured using fluorescence imaging, allowing the study of the evolution of the imbalance $\mathcal{I}$ between the initially occupied and unoccupied halves. With no or weak disorder, $\mathcal{I}$ vanished within times accessible experimentally, i.e., it attained the value expected in thermal equilibrium. But beyond a certain disorder strength, $\mathcal{I}$ appeared to saturate to a nonzero value. This saturation was taken as evidence for MBL [28].

Features of the experimental setup in Ref. [28] can lead to a very slow equilibration of $\mathcal{I}$ to the point of making it difficult to distinguish glassy behavior from the MBL phase. First, the initial dynamics in the unoccupied half of the trap is dominated by Anderson physics (because of low site occupation). The second feature sets in at longer times. The initial MI, before the removal of the bosons in one half of the system, is close in energy to the ground state after the lattice depth is lowered but the system remains deep in the MI regime. The MI, in turn, is close in energy to a BG with a site occupancy slightly below one at the same interaction strength (if the disorder is strong enough to generate a BG). Therefore, the dynamics resulting from the gradual decrease of the site occupations in the occupied half of the system, after the removal of the bosons in the other half, can be dominated by excitations of the BG in the remaining half.

To study the impact of glassy physics we use GMFT to model the dynamics of the experiments in Ref. [28]. GMFT provides qualitatively correct phase diagrams for strongly interacting clean [40–43] and disordered [44–48] (away from the tip of the Mott lobe) systems. It has also been used to study non-equilibrium effects such as the dynamical generation of molecular condensates [49] and MIs [50], dipole oscillations [51], quantum quenches [48, 52, 53], expansion dynamics [54, 55], and transport in the presence of disorder [48, 56]. However, since the Gutzwiller ansatz wavefunction is a product state, it has zero entanglement entropy for any partitioning of the system. GMFT is therefore capable of capturing BG dynamics but it cannot capture thermalization and MBL phases [57], which after taken out of equilibrium, e.g., using a quantum quench, exhibit a linear [58] and logarithmic [59] growth of the entanglement entropy, respectively, with time.

We use GMFT to study the dynamics of initial states under the same (or similar) conditions as the experiment thus allowing direct comparison. We find that the GMFT dynamics is similar but not quite the same as that in the experiment. In particular, the GMFT state rebalances more slowly, which motivates us to add a phenomenological parameter to our theory to gradually remove slow particles from data analysis because they are not accurately captured by our theory. A single phenomenological parameter significantly improves the agreement between

theory and experiment.

Given the fact that GMFT cannot describe dynamics in an MBL phase, our results raise concerns as to whether experimental observations are the result of MBL or the result of slow transport due to glassy dynamics. Only the latter is captured by our GMFT treatment.

Model: We consider bosons in a 2D square lattice subjected to disorder and a parabolic trapping potential, as described by the Bose-Hubbard Hamiltonian:

$$\hat{H} = -J \sum_{\langle \mathbf{ij} \rangle} \hat{b}_{\mathbf{i}}^{\dagger} \hat{b}_{\mathbf{j}} + \frac{U}{2} \sum_{\mathbf{i}} \hat{n}_{\mathbf{i}} (\hat{n}_{\mathbf{i}} - 1) + \sum_{\mathbf{i}} \mu_{\mathbf{i}} \hat{n}_{\mathbf{i}}, \quad (1)$$

where $\hat{b}_{\mathbf{i}}^{\dagger}$ creates a boson at site $\mathbf{i} \equiv (i_x, i_y)$ and $\hat{n}_{\mathbf{i}} = \hat{b}_{\mathbf{i}}^{\dagger} \hat{b}_{\mathbf{i}}$ is the site occupation operator. J parametrizes the tunneling between nearest-neighbor and U is the on-site repulsive interaction. The chemical potential (μ), harmonic trap (of strength Ω), and disorder potential ($\epsilon_{\mathbf{i}}$) are in $\mu_{\mathbf{i}} = -\mu + \Omega |\mathbf{i} - \mathbf{r}_0|^2 + \epsilon_{\mathbf{i}}$, with $\mathbf{r}_0 = (0,0)$ chosen in the center of 4 sites. We focus on a lattice with 31×31 sites in which, for the Hamiltonian parameters used here, the sites at the edges are always empty. We consider two types of disorder, with uniform and Gaussian distributions, whose strengths are denoted by Δ_u and Δ_g, respectively. We set $k_B = \hbar = 1$.

Methods: We study the dynamics of zero and nonzero temperature initial states. The density matrix within GMFT is:

$$\hat{\rho}(t) = \prod_{\mathbf{i}} \hat{\rho}_{\mathbf{i}}(t) = \prod_{\mathbf{i}} \left[\sum_{m,n=0}^{\infty} \alpha_{mn}^{(\mathbf{i})}(t) |m\rangle_{\mathbf{i}} \,_{\mathbf{i}}\langle n| \right], \quad (2)$$

where $|n\rangle_{\mathbf{i}}$ is the state with n bosons at site $\mathbf{i}$, and t denotes time. This ansatz decouples Eq. (1) into single-site Hamiltonians: $\hat{H}_{\mathbf{i}}^{\mathrm{MF}} = -J(\phi_{\mathbf{i}}^* \hat{b}_{\mathbf{i}} + \phi_{\mathbf{i}} \hat{b}_{\mathbf{i}}^{\dagger}) + (U/2) \sum_{\mathbf{i}} \hat{n}_{\mathbf{i}} (\hat{n}_{\mathbf{i}} - 1) + \mu_{\mathbf{i}} \hat{n}_{\mathbf{i}}$, where $\phi_{\mathbf{i}} = \sum_{\mathbf{j} \in \mathrm{nn}_{\mathbf{i}}} \mathrm{Tr}(\hat{\rho}_{\mathbf{j}} \hat{b}_{\mathbf{j}})$ sums over neighbor sites to $\mathbf{i}$. Substituting Eq. (2) into the von Neumann equation, $i \partial_t \hat{\rho} = [\hat{H}, \hat{\rho}]$, leads to the equation of motion for $\alpha_{mn}^{(\mathbf{i})}$:

$$\begin{aligned} i \partial_t \alpha_{m,n}^{(\mathbf{i})} = &-J \phi_{\mathbf{i}}^* \left[\sqrt{m+1} \alpha_{m+1,n}^{(\mathbf{i})} - \sqrt{n} \alpha_{m,n-1}^{(\mathbf{i})} \right] \\ &- J \phi_{\mathbf{i}} \left[\sqrt{m} \alpha_{m-1,n}^{(\mathbf{i})} - \sqrt{n+1} \alpha_{m,n+1}^{(\mathbf{i})} \right] \\ &+ \frac{U}{2} \left[m(m-1) - n(n-1) \right] \alpha_{m,n}^{(\mathbf{i})} \\ &+ \mu_{\mathbf{i}} (m-n) \alpha_{m,n}^{(\mathbf{i})}, \end{aligned} \quad (3)$$

which yields the time evolution of the site occupations: $n_{\mathbf{i}}(t) = \mathrm{Tr}(\hat{\rho}_{\mathbf{i}} \hat{n}_{\mathbf{i}})$.

Following Ref. [28], we quantify the degree of localization using the imbalance:

$$\mathcal{I}(t) = \frac{N_L(t) - N_R(t)}{N_L(t) + N_R(t)}, \quad (4)$$

where $N_L(t) = \sum_{-l_x \leq i_x < i_0, |i_y| \leq l_y} n_{i_x, i_y}(t)$ and $N_R(t) = \sum_{i_0 \leq i_x \leq l_x, |i_y| \leq l_y} n_{i_x, i_y}(t)$, with an $l_x \times l_y$ central region
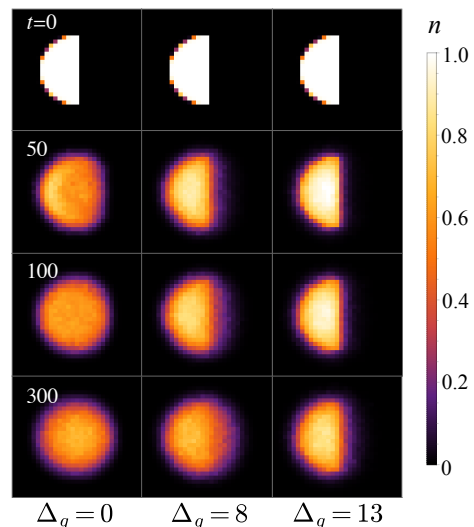

Figure 1. The site occupations for quenched dynamics at zero temperature. Columns (rows) depict results for different disorder strengths (different times). At time $t = 0$ all bosons in the right half of the system are removed and the remainder evolves for $t > 0$. The $t = 0$ state is the ground state for a very small hopping and no disorder. For $t > 0$, Gaussian disorder of strength Δ_g is introduced and the hopping is increased. The state evolves for $t \geq 0$ with no parameter changes.

of interest. l_y is taken to be 2 to define a window 5 lattice sites wide in the y direction. We first set l_x to $l_W = 9$, as in experiment. In Ref. [28], the lattice center does not always coincide with the center of the harmonic potential, and this causes an imperfect preparation of the the initial state domain wall. To account for this, the line separating the left and right sides of the system is defined using $i_0 = 0$ or $i_0 = 1$. The imbalance is obtained by averaging the two cases.

We also compute the inverse decay length, $\lambda(t)$ [28]. To calculate $\lambda(t)$ we first compute the average: $\bar{n}_{i_x}(t) = (2l_y + 1)^{-1} \sum_{|i_y| \leq l_y} n_{i_x, i_y}(t)$. λ is then obtained by fitting:

$$\bar{n}_{i_x}(t) / \bar{n}_{i_x}^0 \sim e^{-\lambda(t) i_x}, \quad (5)$$

where $\bar{n}_{i_x}^0$ is the zero disorder steady-state density and i_x denotes a least squares fit from $i_x = 0$ to l_x.

For $\hat{\rho}(t = 0)$, we take the ground state or a thermal state of the initial Hamiltonian, such that $\hat{\rho}_{\mathbf{i}} = Z_{\mathbf{i}}^{-1} e^{-\beta \hat{H}_{\mathbf{i}}^{\mathrm{MF}}}$ (where $\beta = 1/T$ is the inverse temperature and $Z_{\mathbf{i}}$ is the partition function). Our calculations in the presence of disorder are done for an ensemble of disorder realizations. Disorder-averaging over around 100 disorder realizations is sufficient for convergence.

Within GMFT, dynamics occur only when there are non-vanishing values of the order parameter $\phi_{\mathbf{i}}$ [see Eq. (3)]. As a result, a pure MI state would exhibit no dynamics within GMFT. We find that, as in Refs. [55, 56], the small region with a non-vanishing order parameter generated by the harmonic trap at the edge of MI do-
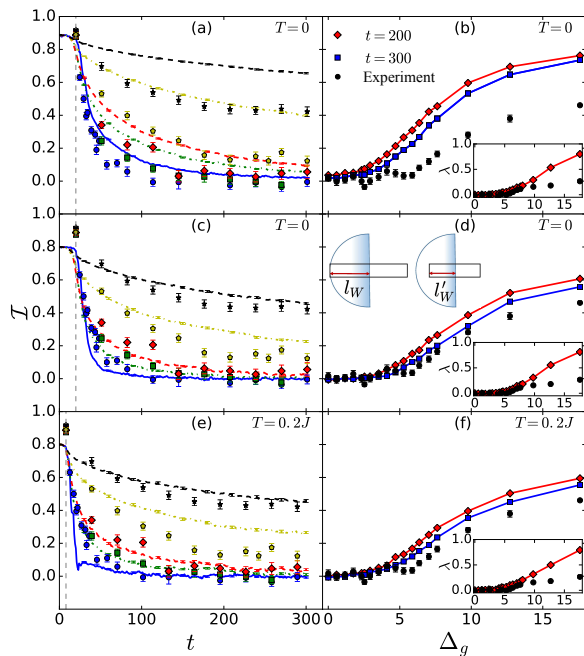
Figure 2. (a): Time evolution of the imbalance $\mathcal{I}$ for various disorder strengths at initial temperature $T = 0$. Lines show simulation results while points with error bars show experimental data [28]. The vertical dashed line marks a time $t^* = 20$ below which $\mathcal{I}$ barely changes within GMFT. The experimental results are shifted to start at t^*. From bottom to top the lines and symbols correspond to $\Delta_g = 0, 3, 4, 8$, and 13. (b): Corresponding $\mathcal{I}$ for the same parameters but at times $t = 200$ and 300 against disorder strength. The experimental result after an evolution time of 187 are also plotted. The inset shows the inverse decay length [Eq. (5)] from our calculation at $t = 200$ and for the experiment after an evolution time $t = 187$. (c) and (d): The same as (a) and (b) but with an analysis window resized from $l_W = 9$ [as in (a) and (b) following Ref. [28]] to $l'_W = 5$, as shown in the schematic. (e) and (f): The same as (c) and (d) but at non-zero temperature. Here t^* reduces to 8.

mains is sufficient to drive dynamics. Remarkably, we will see that the ensuing dynamics measured by imbalance is slower but similar to that in the experiments [28] at long times. We will then show that decreasing l_x to phenomenologically remove particles in the MI state significantly improves agreement with experiment.

Quenched dynamics: In the experiment [28] the dynamics took place after lowering the lattice depth and introducing a disorder potential to a MI created in a deep lattice and to which all atoms in one half of the system were removed. From now on, we use the hopping parameter after the quench $J = U/24.4$ as our energy unit. To create the initial state, we used the experimental parameters [28]: $J_I = 0.244$, $U = 24.4$, $\Omega = 0.145$, and $\mu = 10.6$. After free energy minimization, particles on the right half of the system are manually removed [by setting $\alpha_{m,n}^{(i_x > 0)} = \delta_{m,0}\delta_{n,0}$ in Eq. (2)], leaving behind a particle

number comparable with the experiment, $N_b \approx 123$. In accordance with the experimental protocol [28], to generate disorder (at the evolution stage) we square a two-dimensional array of uniformly distributed random numbers followed by a convolution with a Gaussian profile of standard deviation 0.5. The disorder strength Δ_g is defined as the full width at half maximum of the resulting disorder profile.

The first column in Fig. 1 depicts the evolution of the site occupations in the absence of disorder. Here the particles expand to reach a steady state with no imbalance. When disorder of strength $\Delta_g = 8$ is introduced, the motion slows considerably and an imbalance remains at the latest time shown. For very strong disorder ($\Delta_g = 13$), the particles remain almost entirely in the initially occupied region.

To quantitatively understand the dynamics, we plot the imbalance against time in Fig. 2(a). For $t < t^*$, the imbalance barely changes. This is an artifact of GMFT for the initial state, which is mostly a MI domain. Beyond t^*, $\mathcal{I}$ vanishes rapidly in the clean limit and for weak disorder. But, as the disorder strength increases, it takes longer for $\mathcal{I}$ to reach the expected $\mathcal{I} = 0$ steady state value. In Fig. 2(a), we also plot the experimental results taking t^* to be the starting time for the experiments. The GMFT and experimental results exhibit good agreement for weak disorder strength, but the latter exhibit faster relaxation as the disorder strength is increased.

In Fig. 2(b), we plot the imbalance alongside experimental results [28], as a function of the disorder strength. In our theoretical results, the upturn in $\mathcal{I}$ vs. Δ_g moves toward stronger disorder strengths as t increases. A similar trend was seen in experiments for $t \lesssim 200$, but the experimental results appeared to saturate for $200 \lesssim t \lesssim 300$. For any given selected time, the upturn in $\mathcal{I}$ vs. Δ_g occurs at a smaller value of Δ_g in GMFT when compared to the experiments, which is expected given the slower dynamics of the former seen in Fig. 2(a).

λ offers another way to quantify the degree of localization by parameterizing the extent to which disorder suppresses the relaxation of site occupations. The inset in Fig. 2(b) shows λ versus Δ_g for $t = 200$ and the experimental results for $t = 187$. The behavior of λ (inset) is similar to that of $\mathcal{I}$ (main panel).

There are also differences between GMFT and experiments. For example, at weak disorder strengths, the experimental data of Fig. 2(b) exhibits oscillations not captured by GMFT. These oscillations in turn impact the comparison of the nature of upturns of $\mathcal{I}$ or λ near $\Delta_g = 5.5$, as they make it look sharper in the experimental results.

A key observable in identifying localization is the time derivative of the imbalance, $\dot{\mathcal{I}}$, at long times, as used in observations of Anderson localization with ultracold atoms [7–12]. The vanishing of $\dot{\mathcal{I}}$ at long times (and in large system sizes) is a necessary condition for local-
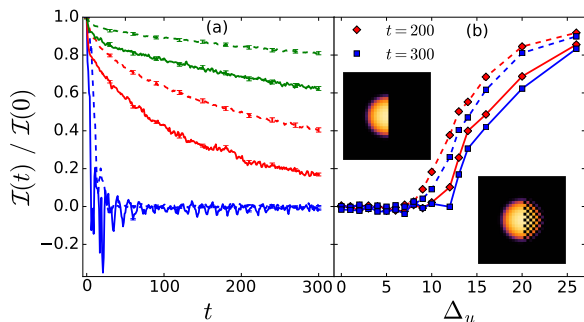
Figure 3. The solid (dashed) lines plot the normalized imbalance where the right half of the trap was initialized to a checkerboard (empty) pattern as shown in the insets. (a) The normalized imbalance against time for various disorder strengths. The pairs of (solid/dashed) lines correspond to uniform disorder $\Delta_u = 0, 13$ and 20 from bottom to top. (b) The normalized imbalance at times $t = 200$ and 300 against disorder strength. The other parameters are $U = 24.4$, $\Omega = 0.145$, and $\mu = 4$.

ization. The slope of $\mathcal{I}$ versus t obtained for the 4 latest experimental times reported is $-1.017(\pm 1.028) \times 10^{-4}$ for the largest disorder strength. Here we see that the experimental error is too large to definitively show a vanishing of the slope since the results are also consistent with just a small slope. Within GMFT, we find a small non-zero slope: $-4.433(\pm 0.053) \times 10^{-4}$, for the largest disorder strength. The small non-zero slope shows that a slow rebalancing (as expected in the glassy state captured within GMFT) is consistent with experiment. Measurements with smaller error bars and time scales much longer than experimentally relevant time scales (such as the trap and light scattering) would allow more direct comparisons.

To understand the robustness of our findings within GMFT, we have also studied initial states at finite temperatures, different quench protocols, and dynamics in the presence of a uniform disorder distribution. The supplementary material shows that the latter two changes do not have much impact on the imbalance dynamics at long times. GMFT shows that the imbalance dynamics of a BG or MI quenched into a disorder profile respond in nearly the same way.

Phenomenological parameter: To improve comparison with experiment we introduce a phenomenological parameter that excludes particles which move too slowly within GMFT. GMFT underestimates the speed of the MI under an applied field. The motion of the entire trapped system is therefore slower than GMFT at long times.

To account for the slow Mott particles we introduce a phenomenological parameter to our GMFT analysis. The inset of Fig. 2(d) shows a schematic of a resizing of the window used to compute the imbalance. The rectangles in the schematics indicate a decrease in l_x in Eq. 4,

from l_W to l'_W. Our phenomenological parameter, l_x, therefore increases the relative rate of rebalancing because slow moving Mott particles near the left edge of the system are excluded in the data analysis. Decreasing μ also removes these particles. We find that tuning either μ or l_x allows us to fit $\mathcal{I}$ versus t to experimental values with the same accuracy. We choose l_x as our phenomenological parameter and vary it to obtain a best fit for the largest disorder, $\Delta_g = 13$.

Figures 2(c) and 2(d) plot the same as panels (a) and (b) but with the new window size, l'_W. Here there is much better agreement with experiment because the relative fraction of mobile to localized particles in our GMFT is closer to experiment. Panels (e) and (f) include non-zero temperature. In varying T we find little change for $T < J$. $T = 0.2J$ was chosen as a best fit for the largest disorder. In Fig. 2(e) we see that t^* diminishes and the imbalance tends to level off quicker at long times, with a slight increase in the slope to $-4.816(\pm 0.160) \times 10^{-4}$.

The comparisons between theory and experiment in Fig. 2 show that by adjusting a single phenomenological parameter we can bring GMFT into better agreement with experiments. We therefore conclude that the long-time relaxation found in experiments can be interpreted within GMFT as glassy dynamics consistent with the out of equilibrium properties of a BG and its excitations.

Checkerboard case: The initial expansion of bosons in the empty half of the trap in the presence of disorder is expected to be dominated by Anderson physics, due to the low site occupations. In order to test how enhancing interactions by increasing site occupations affects the expansion, we have devised an "improved" initial state generated by emptying sites in one half of the system according to a checkerboard pattern. The dynamics then proceeds by allowing the remaining bosons to evolve without any change in the Hamiltonian parameters (no parameter quenching). Before emptying sites, the system was in the ground state.

Fig. 3 plots the normalized imbalance for the checkerboard pattern. The pattern speeds up the decay of $\mathcal{I}(t)/\mathcal{I}(0)$ by enhancing the effect of interactions during the dynamics. It would be interesting to find out how changes in the pattern used for the initial state change the results in the experiments [28].

Discussion: Motivated by Ref. [28], we have studied the dynamics of bosons in 2D lattices with disorder by GMFT. We showed that theory becomes closer to experiment by including temperature and a single phenomenological parameter. We also showed that the features observed in the experiments are robust for various initial states: quenched MI, disordered superfluid, and BG. Since GMFT misses the entanglement present in MBL phases, *evidence for MBL must lie in the differences between GMFT and experiments.* We find that at the present stage with only the data from Ref. [28], it is difficult to tell if there is a qualitative or quantitative

difference between GMFT and experiments. Further experiments, particularly at longer times, will be needed to unambiguously show that MBL is occurring. Avoiding macroscopic mass transport, as done in Ref. [27], will help rule out slow dynamics due to Anderson and BG physics.

––––––––––

[1] P. Verkerk, B. Lounis, C. Salomon, C. Cohen-Tannoudji, J.-Y. Courtois, and G. Grynberg, "Dynamics and spatial order of cold cesium atoms in a periodic optical potential," Phys. Rev. Lett. **68**, 3861 (1992).

[2] P. S. Jessen, C. Gerz, P. D. Lett, W. D. Phillips, S. L. Rolston, R. J. C. Spreeuw, and C. I. Westbrook, "Observation of quantized motion of rb atoms in an optical field," Phys. Rev. Lett. **69**, 49–52 (1992).

[3] A. Hemmerich and T. W. Hansch, "Two-dimesional atomic crystal bound by light," Phys. Rev. Lett. **70**, 410 (1993).

[4] I. Bloch, J. Dalibard, and W. Zwerger, "Many-body physics with ultracold gases," Rev. Mod. Phys. **80**, 885 (2008).

[5] M. A. Cazalilla, R. Citro, T. Giamarchi, E. Orignac, and M. Rigol, "One dimensional bosons: From condensed matter systems to ultracold gases," Rev. Mod. Phys. **83**, 1405 (2011).

[6] M. Köhl, H. Moritz, T. Stöferle, K. Günter, and T. Esslinger, "Fermionic atoms in a three dimensional optical lattice: Observing Fermi surfaces, dynamics, and interactions," Phys. Rev. Lett. **94**, 080403 (2005).

[7] J. Billy, V. Josse, Z. Zuo, A. Bernard, B. Hambrecht, P. Lugan, D. Clément, L. Sanchez-Palencia, P. Bouyer, and A. Aspect, "Direct observation of Anderson localization of matter waves in a controlled disorder," Nature **453**, 891 (2008).

[8] G. Roati, C. D'Errico, L. Fallani, M. Fattori, C. Fort, M. Zaccanti, G. Modugno, M. Modugno, and M. Inguscio, "Anderson localization of matter waves in a Bose-Einstein condensate," Nature **453**, 895 (2008).

[9] J. Chabé, G. Lemarié, B. Grémaud, D. Delande, P. Szriftgiser, and J. C. Garreau, "Experimental observation of the Anderson metal-insulator transition with atomic matter waves," Phys. Rev. Lett. **101**, 255702 (2008).

[10] G. Lemarié, J. Chabé, P. Szriftgiser, J.C. Garreau, B. Grémaud, and D. Delande, "Observation of the Anderson metal-insulator transition with atomic matter waves: Theory and experiment," Phys. Rev. A **80**, 043626 (2009).

[11] S. S. Kondov, W. R. McGehee, J. J. Zirbel, and B. DeMarco, "Three-dimensional Anderson localization of ultracold matter," Science **334**, 66 (2011).

[12] F. Jendrzejewski, A. Bernard, K. Mulller, P. Cheinet, V. Josse, M. Piraud, L. Pezze, L. Sanchez-Palencia, A. Aspect, and P. Bouyer, "Three-dimensional localization of ultracold atoms in an optical disordered potential," Nat. Phys. **8**, 398 (2012).

[13] M. Greiner, O. Mandel, T. Esslinger, T. W. Hansch, and I. Bloch, "Quantum phase transition from a superfluid to a Mott insulator in a gas of ultracold atoms," Nature **415**, 39 (2002).

[14] T. Stöferle, H. Moritz, C. Schori, M. Köhl, and T. Esslinger, "Transition from a strongly interacting 1d superfluid to a Mott insulator," Phys. Rev. Lett. **92**, 130403 (2004).

[15] I. B. Spielman, W. D. Phillips, and J. V. Porto, "Mott-insulator transition in a two-dimensional atomic Bose gas," Phys. Rev. Lett. **98**, 080404 (2007).

[16] R. Jordens, N. Strohmaier, K. Guenther, H. Moritz, and T. Esslinger, "A Mott insulator of fermionic atoms in an optical lattice," Nature **455**, 204 (2008).

[17] U. Schneider, L. Hackermueller, S. Will, T. Best, I. Bloch, T. A. Costi, R. W. Helmes, D. Rasch, and A. Rosch, "Metallic and insulating phases of repulsively interacting fermions in a 3D optical lattice," Science **322**, 1520 (2008).

[18] Y. P. Chen, J. Hitchcock, D. Dries, M. Junker, C. Welford, and R. G. Hulet, "Phase coherence and superfluid-insulator transition in a disordered Bose-Einstein condensate," Phys. Rev. A **77**, 033632 (2008).

[19] M. White, M. Pasienski, D. McKay, S. Q. Zhou, D. Ceperley, and B. DeMarco, "Strongly interacting bosons in a disordered optical lattice," Phys. Rev. Lett. **102**, 055301 (2009).

[20] M. Pasienski, D. McKay, M. White, and B. DeMarco, "A disordered insulator in an optical lattice," Nat. Phys. **6**, 677 (2010).

[21] B. Gadway, D. Pertot, J. Reeves, M. Vogt, and D. Schneble, "Glassy behavior in a binary atomic mixture," Phys. Rev. Lett. **107**, 145306 (2011).

[22] M. C. Beeler, M. E. W. Reed, T. Hong, and S. L. Rolston, "Disorder-driven loss of phase coherence in a quasi-2D cold atom system," New J. Phys. **14**, 073024 (2012).

[23] J.-P. Brantut, J. Meineke, D. Stadler, S. Krinner, and T. Esslinger, "Conduction of ultracold fermions through a mesoscopic channel," Science **337**, 1069 (2012).

[24] L. Tanzi, E. Lucioni, S. Chaudhuri, L. Gori, A. Kumar, C. D'Errico, M. Inguscio, and G. Modugno, "Transport of a Bose gas in 1D disordered lattices at the fluid-insulator transition," Phys. Rev. Lett. **111**, 115301 (2013).

[25] S. Krinner, D. Stadler, J. Meineke, J. P. Brantut, and T. Esslinger, "Superfluidity with disorder in a thin film of quantum gas," Phys. Rev. Lett. **110**, 100601 (2013).

[26] S. S. Kondov, W. R. McGehee, W. Xu, and B. DeMarco, "Disorder-induced localization in a strongly correlated atomic Hubbard gas," Phys. Rev. Lett. **114**, 083002 (2015).

[27] M. Schreiber, S. S. Hodgman, P. Bordia, H. P. Lüschen, M. H. Fischer, R. Vosk, E. Altman, U. Schneider, and I. Bloch, "Observation of many-body localization of interacting fermions in a quasirandom optical lattice," Science **349**, 842 (2015).

[28] Jae-yoon Choi, Sebastian Hild, Johannes Zeiher, Peter Schaus, Antonio Rubio-Abadal, Tarik Yefsah, Vedika Khemani, David A. Huse, Immanuel Bloch, and Christian Gross, "Exploring the many-body localization transition in two dimensions," Science **352**, 1547 (2016).

[29] M. P. A. Fisher, P. B. Weichman, G. Grinstein, and D. S. Fisher, "Boson localization and the superfluid-insulator transition," Phys. Rev. B **40**, 546 (1989).

[30] R. T. Scalettar, G. G. Batrouni, and G. T. Zimanyi, "Localization in interacting, disordered, bose systems," Phys. Rev. Lett. **66**, 3144 (1991).

[31] D. M. Basko, I. L. Aleiner, and B. L. Altshuler, "Metal-insulator transition in a weakly interacting many-electron system with localized single-particle states," Ann. Phys. **321**, 1126 (2006).

[32] V. Oganesyan and D. A. Huse, "Localization of interacting fermions at high temperature," Phys. Rev. B **75**, 155111 (2007).

[33] A. Pal and D.A. Huse, "Many-body localization phase transition," Phys. Rev. B **82**, 174411 (2010).

[34] J. M. Deutsch, "Quantum statistical mechanics in a closed system," Phys. Rev. A **43**, 2046 (1991).

[35] M. Srednicki, "Chaos and quantum thermalization," Phys. Rev. E **50**, 888 (1994).

[36] M. Rigol, V. Dunjko, and M. Olshanii, "Thermalization and its mechanism for generic isolated quantum systems," Nature **452**, 854 (2008).

[37] R. Nandkishore and D. A. Huse, "Many-body localization and thermalization in quantum statistical mechanics," Annu. Rev. Condens. Matter Phys. **6**, 15 (2015).

[38] V. W. Scarola and B. DeMarco, "Dynamics of hubbard-band quasiparticles in disordered optical lattices," Phys. Rev. A **92**, 053628 (2015).

[39] R. Mondaini and M. Rigol, "Many-body localization and thermalization in disordered hubbard chains," Phys. Rev. A **92**, 041601 (2015).

[40] D. S. Rokhsar and B. G. Kotliar, "Gutzwiller projection for bosons," Phys. Rev. B **44**, 10328 (1991).

[41] D. Jaksch, C. Bruder, J. I. Cirac, C. W. Gardiner, and P. Zoller, "Cold bosonic atoms in optical lattices," Phys. Rev. Lett. **81**, 3108 (1998).

[42] I. Hen and M. Rigol, "Superfluid to Mott insulator transition of hardcore bosons in a superlattice," Phys. Rev. B **80**, 134508 (2009).

[43] I. Hen, M. Iskin, and M. Rigol, "Phase diagram of the hard-core Bose-Hubbard model on a checkerboard superlattice," Phys. Rev. B **81**, 064503 (2010).

[44] K. Sheshadri, H. R. Krishnamurthy, R. Pandit, and T. V. Ramakrishnan, "Percolation-enhanced localization in the disordered bosonic Hubbard model," Phys. Rev. Lett. **75**, 4075 (1995).

[45] B. Damski, J. Zakrzewski, L. Santos, P. Zoller, and M. Lewenstein, "Atomic Bose and Anderson glasses in optical lattices," Phys. Rev. Lett. **91**, 080403 (2003).

[46] P. Buonsante, V. Penna, A. Vezzani, and P. B. Blakie, "Mean-field phase diagram of cold lattice bosons in disordered potentials," Phys. Rev. A **76**, 011602 (2007).

[47] P. Buonsante, F. Massel, V. Penna, and A. Vezzani, "Gutzwiller approach to the Bose-Hubbard model with random local impurities," Phys. Rev. A **79**, 013623 (2009).

[48] C. H. Lin, R. Sensarma, K. Sengupta, and S. Das Sarma, "Quantum dynamics of disordered bosons in an optical lattice," Phys. Rev. B **86**, 214207 (2012).

[49] D. Jaksch, V. Venturi, J. I. Cirac, C. J. Williams, and P. Zoller, "Creation of a molecular condensate by dynamically melting a Mott insulator," Phys. Rev. Lett. **89**, 040402 (2002).

[50] J. Zakrzewski, "Mean field dynamics of superfluid-insulator phase transition in a gas of ultra cold atoms," Phys. Rev. A **71**, 043601 (2005).

[51] M. Snoek and W. Hofstetter, "Two-dimensional dynamics of ultracold atoms in optical lattices," Phys. Rev. A **76**, 051603 (2007).

[52] F. A. Wolf, I. Hen, and M. Rigol, "Collapse and revival oscillations as a probe for the tunneling amplitude in an ultracold Bose gas," Phys. Rev. A **82**, 043601 (2010).

[53] M. Snoek, "Rigorous mean-field dynamics of lattice bosons: Quenches from the Mott insulator," Europhys. Lett. **95**, 30006 (2011).

[54] I. Hen and M. Rigol, "Analytical and numerical study of trapped strongly correlated bosons in two- and three-dimensional lattices," Phys. Rev. A **82**, 043634 (2010).

[55] M. Jreissaty, J. Carrasquilla, F. A. Wolf, and M. Rigol, "Expansion of Bose-Hubbard Mott insulators in optical lattices," Phys. Rev. A **84**, 043610 (2011).

[56] M. Yan, H.-Y. Hui, and V. W. Scarola, "Dynamics of disordered states in the Bose-Hubbard model with confinement," (2016), arXiv:1601.06817.

[57] B. Bauer and C. Nayak, "Area laws in a many-body localized state and its implications for topological order," J. Stat. Mech: Theory Exp. **2013**, P09005 (2013).

[58] H. Kim and D. A. Huse, "Ballistic spreading of entanglement in a diffusive nonintegrable system," Phys. Rev. Lett. **111**, 127205 (2013).

[59] J. H. Bardarson, F. Pollmann, and J. E. Moore, "Unbounded growth of entanglement in models of many-body localization," Phys. Rev. Lett. **109**, 017202 (2012).